

# **A TOP-DOWN SCALING ANALYSIS FOR THE ROSA-IV/LSTF INTEGRAL EFFECTS TEST FACILITY TO SUPPORT APPLYING THE WCOBRA/TRAC-TF2 SYSTEM CODE TO A THREE-LOOP PWR SMALL BREAK LOCA**

**Jun Liao and Katsuhiro Ohkawa**

LOCA Integrated Services I, Westinghouse Electric Company  
1000 Westinghouse Drive, Cranberry Township, PA 16066, USA  
liaoj@westinghouse.com

## **ABSTRACT**

The FULL SPECTRUM™ LOCA (FSLOCA™) evaluation model, which utilized WCOBRA/TRAC-TF2 system code, is the latest Westinghouse LOCA evaluation model for analyzing both large break LOCA and small break LOCA in PWR. The ROSA-IV integral effects test (IET) facility is the key facility in validation matrix of the WCOBRA/TRAC-TF2 code. The ROSA-IV facility is a 1/48 power/volume scaled IET facility to a four loop Westinghouse PWR, and the scaling factor and scaling distortion have been extensively studied. However, the pilot PWR in Full Spectrum LOCA evaluation model is a three-loop Westinghouse PWR, which leads to different scaling factor and distortions.

Top-down scaling approach evaluates the global system behaviors and system interactions from IETs, and addresses the similarity between the IETs and the prototype PWR. The top-down scaling has been used to investigate scale distortion between the AP600 PWR and the APEX integral effects test facility and between US-APWR and the ROSA-IV integral effects test facility. In this work, the scaling distortion between the ROSA-IV integral effects test facility and a Westinghouse three-loop PWR is investigated using the top-down scaling analysis.

The top-down scaling in the blowdown, natural circulation, loop seal clearing, and boil off phases in a ROSA-IV SB-CL-02 test was investigated relative to the three-loop PWR SBLOCA transient. The top-down scaling analysis results indicated that there are minor scale distortions originating from the atypical steady state and transient initiation of ROSA-IV test. The scale analysis demonstrated that the ROSA-IV tests are well scaled IETs for examining the behavior of Westinghouse three-loop PWRs under the SBLOCA transient conditions, and are uniquely suited for the validation of WCOBRA/TRAC-TF2 for the application to SBLOCA analysis.

## **KEYWORDS**

Top-Down Scaling, PWR, LOCA

## **1. INTRODUCTION**

The FULL SPECTRUM™ loss-of-coolant accident (FSLOCA™) evaluation model [1], which utilized WCOBRA/TRAC-TF2 system code, is the latest Westinghouse LOCA evaluation model for analyzing both large break LOCA and small break LOCA in PWR. The WCOBRA/TRAC-TF2 code consists of a three-dimensional subchannel module in for simulating the reactor vessel and a one-dimensional two-fluid module that is derived from the TRAC-P computer code [2] for the reactor coolant loop and the emergency core cooling system. The three-dimensional sub-channel model is adequate to describe the phenomena expected in the reactor pressure vessel during a LOCA scenario. The two-fluid, six-equation formulation [1] utilized in the one dimensional module is able to describe the reactor coolant system loop phenomena, especially when a characterization of stratified flow is required.

The development of the FSLOCA evaluation model followed the Evaluation Model Development and Assessment Process (EMDAP) which is outlined in the Regulatory Guide (RG) 1.203 [3] and the Standard Review Plan (SRP) discussed in the NUREG-0800 [4]. RG 1.203 describes a structured development and assessment process that is an upgrade from the principles of the CSAU roadmap [5]. There are four elements in

*FULL SPECTRUM™ and FSLOCA™ are trademarks in the United States of Westinghouse Electric Company LLC, its subsidiaries and/or its affiliates. These marks may be used and/or registered in other countries throughout the world. All rights reserved. Unauthorized use is strictly prohibited. Other names may be trademarks of their respective owners.*

EMDAP. Element 1 of the EMDAP process focuses on how to establish the requirements for the Evaluation Model (EM). One key step in the EMDAP process (as well as in the CSAU) is the Phenomena Identification and Ranking Table (PIRT). The process is used to develop the functional requirements for the new evaluation model as well as to define the validation data base. Traditionally, separate PIRTs have been developed by focusing on the LBLOCA or the SBLOCA scenarios as two different entities. An integrated PIRT [1] was developed to span over the full spectrum of break sizes.

Elements 2, 3 and 4 describe a suitable process for the development and the assessment of the evaluation model (EM), sometimes referred to as Verification and Validation (V&V). An assessment matrix is established where Separate Effect Tests (SETs) and Integral Effect Tests (IETs) are selected to validate the code against the important phenomena identified in the PIRT. The code biases and uncertainties are established and the effect of scale determined.

SETs are used to develop and assess groups of empirical correlations and other closure models associated to the important phenomena. The validation in FSLOCA EM [1] includes extensive amount of SETs that covers the major phenomena such as break flow, post-CHF core heat transfer, core void distribution and mixture level, horizontal stratified flow, cold leg condensation, ECC bypass, steam binding, loop seal clearance, etc., in either LBLOCA or SBLOCA.

IETs are used to assess system interactions and global code capability. The LBLOCA assessments of WCOBRA/TRAC-TF2 were mainly performed using large scale test facilities utilized as part of the international 2D/3D program. The facilities included in the code assessment include the Upper Plenum Test Facility (UPTF), and the Cylindrical Core Test Facility (CCTF). LOFT IETs were used to assess the capability of the code to model large break LOCA events with the nuclear core and with the focus to the blowdown stage. The purpose of those assessments was to confirm that the code is able to predict the LBLOCA phenomena with performance similar to the NRC approved code (WCOBRA/TRAC [6]). The integral effect tests assessment for SBLOCA was based on the ROSA test facility (ROSA IV/LSTF) [7] with additional assessment with the LOFT SBLOCA tests.

The EMDAP emphasize on the scaling analysis of the computer code, the closure models, and the IETs and SETs. Specifically, the IET and SET facilities and experimental data are evaluated by the scaling analysis to respond to Step 6 in Element 2 of EMDAP “Perform Scaling Analysis and Identify Similarity Criteria”, to ensure that the test data, and the models based on those data, will be applicable to the full-scale analysis of the plant transient. When the distortions in the IETs arise due to the configuration difference or boundary conditions, the effects of the distortions should be evaluated according to Step 8(a) in Element 2 of EMDAP “Evaluate Effects of IET Distortions and SET Scale up Capability”. Furthermore, the rationale and techniques associated with evaluating scaleup capability of the models or correlations in the computer code should be provided as suggested in Step 8(b) in Element 2 of EMDAP.

Step 15 of Element 4 of EMDAP “Assess Scalability of Models” requires scalability analysis on whether the specific model or correlation is appropriate for application to the configuration and conditions of the plant and transient under evaluation. Step 19 in Element 4 of EMDAP “Assess Scalability of Integrated Calculations and Data for Distortions” is to assess scalability of integrated calculation and data for distortion. This scalability evaluation is limited to whether the assessment calculations and experiments exhibit otherwise unexplainable differences among facilities, or between calculated and measured data for the same facility, which may indicate experimental or code scaling distortions.

The scaling analyses in EMDAP include both top-down and bottom-up approaches. The top-down scaling approach evaluates the global system behavior and systems interactions from integral test facilities that can be shown to represent the plant-specific design under consideration. A top-down scaling methodology is developed and applied to achieve the following purposes:

- (1) Derive the non-dimensional groups governing similitude between facilities.
- (2) Show that these groups scale the results among the experimental facilities.
- (3) Determine whether the ranges of group values provided by the experiment set encompass the corresponding plant- and transient-specific values.

The bottom-up scaling analyses address issues raised in the plant- and transient-specific PIRT related to localized behavior. These analyses are used to explain differences among tests in different experimental facilities and to use

these explanations to infer the expected plant behavior and determine whether the experiments provide adequate plant-specific representation.

The FSLOCA topical report [1] has provided the bottom-up scaling analyses or discussions for the each closure model, separated effects test and integral effects test. This study provides a top-down scaling analysis to evaluate the effect of IET distortions for SBLOCA to satisfy the requirements in Step 8(a) and Step 19 of EMDAP.

There were several integral effects test facility for SBLOCA in PWR, notably, BETHSY, LOBI, LOFT, PKL, ROSA-IV/LSTF, Semiscale, and SPES. Among them, ROSA-IV /LSTF [7] features the largest scale (1/48 power-volume), and prototypical configuration for Westinghouse four-loop PWR, a large test matrix, and state-of-the-art instrumentations. The general structure of the ROSA-IV/LSTF facility is shown in Figure 1. It is a full height test facility, but the four loops in the prototypical PWRs are simplified to a broken loop and an intact loop. With the major components such as the reactor pressure vessel and steam generator follows the volumetric scale, the hot leg and cold legs are scaled to keep the similarity of Froude number.

However, the existing ROSA scaling analysis [7][8] focus on the Westinghouse four-loop PWR, while a three-loop Westinghouse PWR (Figure 2) is selected as the pilot PWR of the FULL SPECTRUM LOCA evaluation model, which leads to different scaling factor and distortions. Thus, the development of FSLOCA EM requires a top-down scaling analysis between the ROSA-IV/LSTF test facility and a Westinghouse three-loop PWR to satisfy the scaling requirement of EMDAP. Next, the history of scaling analysis for nuclear experimental facility is reviewed.

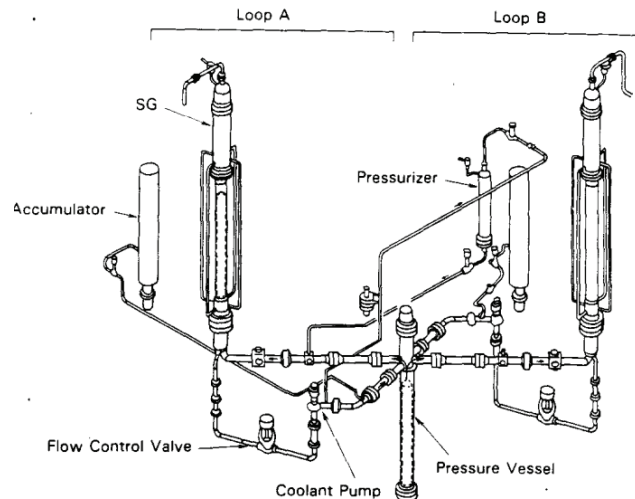


**Figure 1. General structure of ROSA-IV/LSTF [7].**

The  $\Pi$  theorem was established by Buckingham [9] in 1914 and widely used in dimensionless analysis to serve as guide for systematic experimentation in the fluid mechanics community and heat transfer community. With the development of nuclear experimental facility, there were numerous scaling analysis methods established for the nuclear thermal hydraulic analysis. The scaling criteria applied for the design of the reduced height test reactor, LOFT, have been examined by Rose in 1965 [10]. Carbiener and Cudnik [11] developed linear scaling method that requires all linear dimensions reduced by the same proportion. Ishii and Kataoka [12] presented scaling criteria specifically for the cooling loops of pressurized water reactors under single phase and two-phase natural circulation conditions. The volume scaling method, which is adequate for full height and full pressure experimental facility, were developed by Nahavandi et al. [13]. The volume scaling method was utilized to design most of integral effects test facilities, such as ROSA/LSTF, BETHSY, CCTF, and others, that are major validation tests for the development of the reactor safety analysis computer codes. Note the diameter of cold leg and hot leg of those facilities was scaled with the similarity of Froude number to preserve the flow regime [14] instead of volume scaling. The hierarchical two-tiered scaling (H2TS) method was presented by Zuber [15] was recommended for the EMDAP. The H2TS method and its extension has been applied to develop the testing facility for advance passive PWRs [16][17]. Fractional Scaling Analysis (FSA) [16] as an update from the H2TS method could be applied for EMDAP as well.

In this study, the scaling distortion in ROSA-IV/LSTF SBLOCA test [19], SB-CL-02, compared to the SBLOCA in a Westinghouse three-loop PWR was investigated using the top-down scaling method used for AP600 by Banerjee [20,16] and for US-APWR by MHI [8]. The scaling analysis technique first divides the SBLOCA into phases based on the components and governing phenomena as the postulated accident evolves. The conservation equations, resolved to the component level and their interconnections, are derived for the active components in each phase. The equations are then non-dimensionalized and reference parameters are selected such that the dependent variables and their time derivatives, other than the system response of interest, are of order 1. Order of magnitude analysis is then performed for each equation and then between equations, based on the numerical values of the non-dimensional coefficients for each term, with only the large order terms being retained. The resulting equations then contain terms whose impact on key system responses are ordered in terms of the magnitude of the non-dimensional groups multiplying the  $O[1]$  dependent variables. The reduced set of equations and non-dimensional groups in the three-loop Westinghouse PWR SBLOCA transient are compared with the ROSA/LSTF SBLOCA experiment. The scaling distortion is then quantified and discussed.

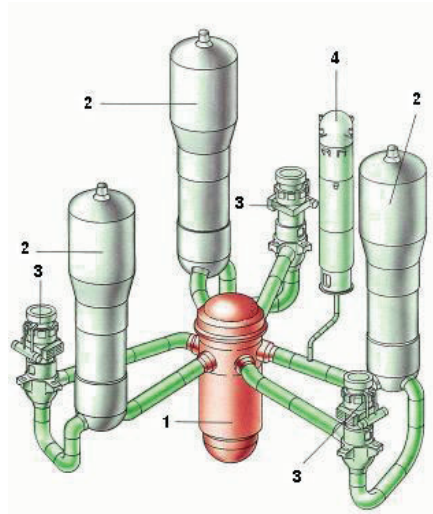


**Figure 2. General structure of a three-loop PWR (1-reactor pressure vessel; 2-steam generator; 3-reactor coolant pump; 4-pressurizer).**

The scaling factor,  $D$ , usually is defined as the ratio of prototype (PWR) to the test facility  $\Pi$ -groups. If the scaling factor is one, the phenomenon is perfectly scaled. The distortion of each phenomenon in this work is quantified using the criteria suggested by Wulff et al. [21]:

- If  $D=1.0$ , the phenomenon is scaled perfectly.
- If  $1/2 < D < 2$  the phenomenon is well scaled
- If  $1/3 < D < 1/2$  or  $2 < D < 3$  the phenomenon presents a distortion of the first grade
- If  $D < 1/3$  or  $D > 3$  the phenomenon presents a distortion of the second grade
- If  $D < 0$  the phenomenon is completely distorted. The distortion acceptability criteria might be different in some cases due to the different normalization of the effect metrics.

In subsequent sections, the SBLOCA scenarios and phases expected in the Westinghouse three-loop PWR are described. Then, the non-dimensional mass and energy equations for the blowdown (BLD), natural circulation (NC), loop seal clearance (LSC), and boil-off (BO) phases are developed. The non-dimensional coefficients from SB-CL-02 and the demonstration plant analysis results were compared for identification and discussion of possible scaling distortions in the ROSA SB-CL-02 experiment.

## 2. SBLOCA SCENARIOS AND PHASE DESCRIPTION

During a postulated small break LOCA, a break occurs at the cold leg of a PWR. The RCS depressurizes to the pressurizer low-pressure setpoint, actuating a reactor trip signal. The ECCS is aligned for delivery following the generation of a safety signal when the pressurizer low-low pressure setpoint is reached. The ECCS includes redundant trains of safety inject into the cold legs. The pressurized accumulators provide additional cold borated water to the RCS in the event of a LOCA. Once sufficient RCS depressurization occurs, accumulator injection commences, which leads to recovery the reactor core.

During a small break LOCA transient, the reactor coolant system depressurizes and coolant mass is lost out the break as the RCS drains to the break elevation, while mass is added from the safety injection (SI) pumps and eventually the accumulators. Water injected by the SI pumps and accumulators must be sufficient so that acceptable core cooling is provided for the spectrum of small break LOCA transients.

The typical scenario of a PWR SBLOCA can be divided into five phases, blowdown, natural circulation, loop seal clearance, boil-off, and core recovery. The duration of each period is break size dependent, and each is characterized as follows:

### Blowdown

On initiation of the break, there is a rapid depressurization of the primary side of the RCS. Reactor trip is initiated on a low pressurizer pressure setpoint. Loss of condenser steam dump effectively isolates the SG secondary side, causing it to pressurize to the safety valve setpoint and release steam through the safety valves. An SI signal occurs when the primary pressure decreases below the pressurizer low-low pressure setpoint, and SI begins after some delay time. The RCS remains nearly liquid solid for most of the blowdown period, with phase separation starting to occur in the upper head, upper plenum, and hot legs near the end of this period. During the blowdown period, the break flow is single-phase liquid. Eventually, the entire RCS saturates, the rapid depressurization ends, and the RCS reaches a pressure just above the SG secondary side pressure.

### Natural Circulation

At the end of the blowdown period, the RCS pressure reaches a quasi-equilibrium condition that can last for several hundred seconds, during which the SG secondary side acts as a heat sink. During this period, the system drains from the top down with voids beginning to form at the top of the SG tubes and continuing to form in the upper head and top of the upper plenum regions. There is still adequate liquid to allow significant natural circulation two-phase flow around the loops; decay heat is removed through condensation in the SGs during this time. Significant coolant mass depletion continues from the RCS, and vapor generated in the core is trapped within the upper regions by liquid plugs in the loop seals, while a low quality flow still exits the break. This period is referred to as the natural circulation period.

### Loop Seal Clearance

The third period is the loop seal clearance period. When the liquid level in the downhill side of the pump suction piping is depressed to the bottom of the loop seal, steam previously trapped in the RCS can be vented to the cold leg break. The break flow, previously a low quality mixture, transitions to primarily steam. Prior to loop seal venting, the static head balances within the RCS can cause the vessel collapsed mixture level to depress into the core. Following the venting, the vessel mixture level recovers to about the cold leg elevation, as the imbalances throughout the RCS are relieved.

### Boil-off

Following loop seal venting, the vessel mixture level continues to decrease due to the boil-off of the remaining liquid inventory since the RCS pressure is generally still too high to allow sufficient ECCS injection by the high pressure SI pumps or the low pressure SI pump. The mixture level will reach a minimum, in some cases resulting in core uncover, before the RCS has depressurized to the point where the break flow is less than the rate at which ECCS water is delivered. This phase is typically ended when accumulator injection commences.

### Core Recovery

The vessel mass inventory is replenished from its minimum with ECCS water (Accumulator and low pressure SI) and the core recovers. The transient is terminated once the entire core is rewetted and the pumped SI flow exceeds the break flow; operator action may facilitate this process.

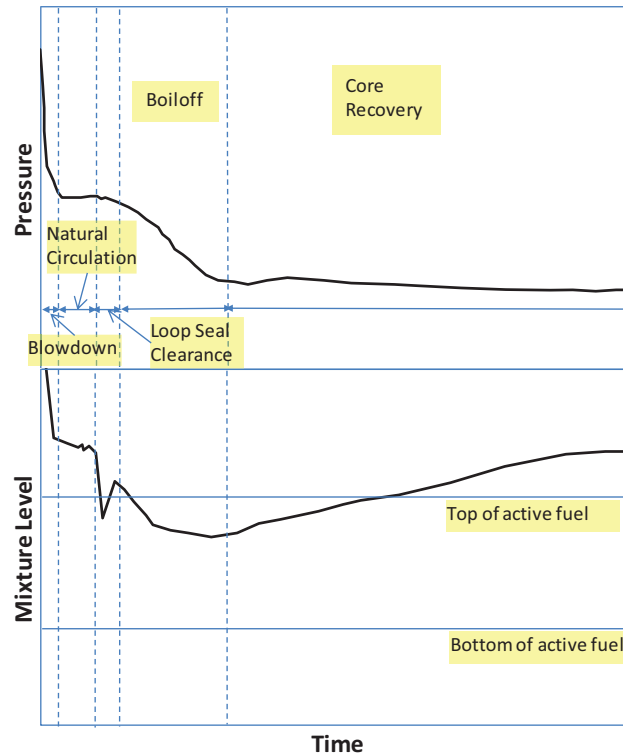


Figure 3. Pressure response and core mixture level in Westinghouse three-loop PWR SBLOCA.

### 3. TOP-DOWN SCALING ANALYSIS FOR ROSA-IV LSFT SB-CL-02

The system pressure and mass transients of three-loop Westinghouse PWR and corresponding ROSA-IV/LSTF were compared for the blowdown, natural circulation, loop seal clearance, and boil-off phases. The limiting cold leg break of Westinghouse three-loop PWR and 2.5% cold leg break SB-CL-02 [22] were selected for this investigation of scale distortion since among all ROSA test series, 2.5% is the closest to the three-loop PWR's limiting break size. Note, there is no high head safety injection in the SB-CL-02 test, and thus the high head safety injection is not assumed in PWR for this top-down scaling analysis. Since ROSA is a full pressure full height facility and the power-volume scaling maintains 1:1 time scale, we can compare the system pressure vs. time directly. The scale distortion in ROSA can be identified through comparison of non-dimensional parameters.

Next, the scaling analysis based on the non-dimensional mass and energy equations for the blowdown, natural circulation, loop seal clearance, and boil-off phases are presented. The non-dimensional coefficients derived from the non-dimensional mass, energy and momentum balance laws were then calculated and compared between the ROSA SB-CL-02 and the three-loop Westinghouse PWR simulation results for identification and discussion of possible scaling distortions in SB-CL-02. To compute the non-dimensional coefficients, the SB-CL-02 simulation and the SBLOCA transient of an equivalent break size are utilized for the parameters not available from the measurements, since the simulation of SB-CL-02 was found to be equivalent to the test in terms of the global mass and pressure transient.



### 3.1. Blowdown phase

In evaluating the global RCS transient behavior of the blowdown phase, the method developed by Banerjee et al. for the AP600 SBLOCA is employed for the basis of this scaling analysis. The reference conditions used to evaluate the dimensionless groups are selected as appropriate for each break size.

The fluid behavior during the blowdown phase in the primary RCS system can be modeled with two fields consisting of a two-phase mixture field and a subcooled liquid field as shown in Figure 4. The two-phase mixture occurs in the core, upper plenum, upper head, hot leg, and steam generator uphill side. The subcooled liquid exists in the steam generator downhill, cross over leg, cold leg, downcomer and lower plenum. The break flow is single-phase liquid discharged from the cold leg. During the blowdown period, the core supplies heat to the two phase mixture and the steam generator absorbs heat from the primary side of RCS.

The governing equations for the blowdown phase are the mass conservation equation and the energy conservation equation. Those equations are non-dimensionalized and a dimensionless pressure rate equation is developed to describe the performance of blowdown phase.

The conservation of mass for each field of the control volume (Figure 4) is written as

$$\frac{d(\rho_k V_k)}{dt} = \sum \dot{m}_{in,k} - \sum \dot{m}_{out,k} \quad (1)$$

Where  $\rho$  is density,  $V$  is volume, and  $\dot{m}_{in}$  and  $\dot{m}_{out}$  are the mass flow rate in and out the field, respectively. Subscript  $k$  denotes each field, subcooled, saturated, etc.

The total mass balance equation for the system, which lumps the saturated field and the subcooled field is given as

$$\frac{dM}{dt} = \sum \dot{m}_{in} - \sum \dot{m}_{out}, \quad (2)$$

where  $M$  is the total mass. The mass exchange in between fields is cancelled out. Eq. (2) can be non-dimensionalized using the reference values for  $M$ ,  $t$ , and the flow rate. Since there is no in flow and the out flow is the flow to the break, the non-dimensional mass conservation equation is shown below.

$$\frac{dM^*}{dt^*} = \Psi_{13} (-\dot{m}_{break}^*), \quad (3)$$

where

$$M^* = M/M_0, \quad (4)$$

$$t^* = t/t_0, \quad (5)$$

$$\dot{m}_{break}^* = \dot{m}_{break}/\dot{m}_{break,0}^*. \quad (6)$$

The subscript of 0 denotes the reference value. The non-dimensional group  $\Psi_{13}$  is defined as

$$\Psi_{13} = \frac{\dot{m}_{break,0}^* t_0}{M_0}. \quad (7)$$

Similar to the mass conservation equation, the energy conservation equation is given:

$$\frac{d(\rho_k V_k u_k)}{dt} = \sum \dot{m}_{in,k} h_{in,k} - \sum \dot{m}_{out,k} h_{out,k} + \dot{q}_{net,k}, \quad (8)$$

where  $u$  is internal energy,  $h$  is the enthalpy, and  $\dot{q}$  is the net heat flux transferred to the field. Note, the kinetic energy and potential energy are ignored in the energy conservation equation for simplicity. For the blowdown phase,

the only path for energy convecting out the system is the mass flow to the break and there is no significant inlet mass flow to the system. The mass conservation equation is given for each field

$$\frac{d(\rho_k V_k)}{dt} = \sum \dot{m}_{in,k} - \sum \dot{m}_{out,k} \quad (9)$$

The left hand side of Eq. (8) is then expanded as

$$\frac{d(\rho_k V_k u_k)}{dt} = \rho_k V_k \frac{du_k}{dt} + u_k \frac{d(\rho_k V_k)}{dt} = \rho_k V_k \frac{du_k}{dt} + u_k (\sum \dot{m}_{in,k} - \sum \dot{m}_{out,k}) \quad (10)$$

Thus, Eq. (8) is re-arranged to obtain the differentiation of the internal energy,

$$\rho_k V_k \frac{du_k}{dt} = \sum \dot{m}_{in,k} (h_{in,k} - u_k) - \sum \dot{m}_{out,k} (h_{out,k} - u_k) + \dot{q}_{net,k} \quad (11)$$

Per thermodynamics relation of mixture

$$h = u + Pv, \quad (12)$$

where  $v$  is specific volume. The pressure is assumed as a function of internal energy and specific volume, thus differentiation of pressure leads to

$$\frac{dP}{dt} = \left. \frac{\partial P}{\partial u} \right|_{v_k} \frac{du}{dt} + \left. \frac{\partial P}{\partial v} \right|_{u_k} \frac{dv}{dt}, \quad (13)$$

The continuity equation of Eq. (9) can be written using specific volume rather than density, which leads to

$$\rho_k V_k \frac{dv_k}{dt} = \frac{dV_k}{dt} - v_k (\sum \dot{m}_{in,k} - \sum \dot{m}_{out,k}) \quad (14)$$

Multiplying Eq. (13) by  $\rho_k V_k$  and substituting Eq. (11) and Eq.(14) for the time derivatives of internal energy and specific volume yields for the pressure rate equation

$$\begin{aligned} \rho_k V_k \frac{dP}{dt} = & \left. \frac{\partial P}{\partial u} \right|_{v_k} (\sum \dot{m}_{in,k} (h_{in,k} - u_k) - \sum \dot{m}_{out,k} (h_{out,k} - u_k) + \dot{q}_{net,k}) \\ & + \left. \frac{\partial P}{\partial v} \right|_{u_k} \left( \frac{dV_k}{dt} - v_k (\sum \dot{m}_{in,k} - \sum \dot{m}_{out,k}) \right) \end{aligned} \quad (15)$$

The pressure difference among multiple fields is small and can be ignored. For the single system pressure, Eq. (15) is summated over the  $k$  fields. With that the total volume of the control volume is a constant, i.e.,  $\sum_k \frac{\partial V_k}{\partial t} = 0$ , the

following equation for the system pressure is obtained,

$$\frac{dP}{dt} = \frac{\sum_k \left. \frac{\partial P}{\partial u_k} \right|_{v_k} (\sum \dot{m}_{in,k} (h_{in,k} - u_k) - \sum \dot{m}_{out,k} (h_{out,k} - u_k) + \dot{q}_{net,k}) - \sum_k v_k (\sum \dot{m}_{in,k} - \sum \dot{m}_{out,k})}{\sum_k \frac{\rho_k V_k}{\left. \frac{\partial P}{\partial v_k} \right|_{u_k}}} \quad (16)$$

For the blowdown in a PWR as shown using control volumes in Figure 4, there are two fields, the subcooled liquid, which is denoted with the subscript of  $l$ , and saturated two-phase mixture, which is denoted with the subscript of  $m$ . Since the only break in this SBLOCA transient is assumed to occur at the cold leg and there is no ECC injection in blowdown, the subcooled fields only discharges flow. Meanwhile, the saturated field has no mass exchange with outside of RCS, but the heat fluxes from the core and steam generator are applied to the saturated mixture. The pressure equation for the blowdown phase is



$$\frac{dP}{dt} = \frac{\frac{\partial P / \partial u_l|_{v_l}}{\partial P / \partial v_l|_{u_l}} (-\dot{m}_{out}(h_{out} - u_m)) + \frac{\partial P / \partial u_m|_{v_m}}{\partial P / \partial v_m|_{u_m}} (\dot{q}_{net}) + v_l \dot{m}_{out}}{\frac{\rho_l V_l}{\partial P / \partial v_l|_{u_l}} + \frac{\rho_m V_m}{\partial P / \partial v_m|_{u_m}}} \quad (17)$$

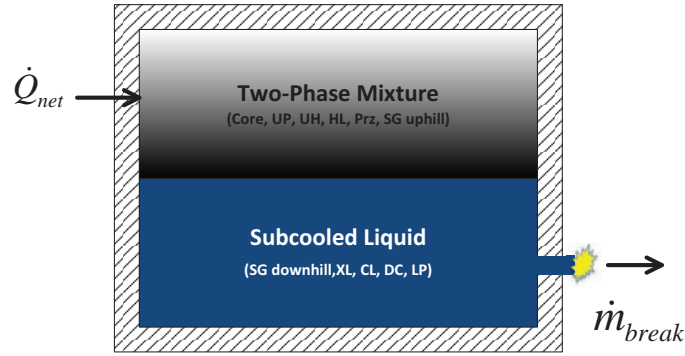


**Figure 4. Schematic of control volume in the blowdown phase.**

Eq. (17) can be non-dimensionalized as

$$\frac{dP^*}{dt^*} = \Psi_2 C_{1,l}^* I_{b,l}^* + \Psi_6 C_{1,m}^* I_{c,m}^* + \Psi_{10} C_2^* \Pi_l^* \quad (18)$$

Definition of non-dimensional coefficients in Eq. (3) and Eq. (18) is given in the following table. The reference time in the analysis is obtained from the transient time of each SBLOCA phase. The reference mass is obtained at the beginning of the phase, and reference mass flow are averaged over the phase. Thus, unlike reference [16], the non-dimensional parameter  $\Psi_{13}$  is not unit across the experiment and PWR. That helps to identify the scaling distortion of the mass inventory in the reactor.

Table I contains the derivatives of pressure with specific internal energy at constant specific volume and the derivative of pressure with specific volume at constant specific internal energy. For the single phase field, it can be obtained using the steam table for subcooled water or steam, or ideal gas equation for the non-condensable gas phase. For the saturated two-phase mixture field, the thermodynamic quality is introduced as another variable. Details of the property calculation refer to references [20] and [23]. A numerical computation can be used to obtain the values of the property derivatives.

**Table I: Definition of Non-dimensional Parameters in the Blowdown Phase**

Non-dimensionalized Parameters	Algebraic form	Note
$M^*$	$M / M_0$	Non-dimensionalized mass
$t^*$	$t / t_0$	Non-dimensionalized time
$\dot{m}_{break}^*$	$\dot{m}_{break} / \dot{m}_{break,0}$	Non-dimensionalized mass flow
$P^*$	$P / P_0$	Non-dimensionalized pressure
$I_{b,l}^*$	$\frac{I_{b,l}}{I_{b,l,0}} = \frac{\dot{m}_{break}(h_{break} - u_l)}{\dot{m}_{break,0}(h_{break} - u_l)_0}$	Non-dimensionalized subcooled field energy change due to mass outflow
$I_{c,m}^*$	$\frac{I_{c,m}}{I_{c,m,0}} = \frac{\dot{q}_{net,m}}{\dot{q}_{net,m,0}}$	Non-dimensionalized heat transfer

$H_l^*$	$\frac{H_l}{H_{l,0}} = \frac{v_l(-\dot{m}_{break})}{v_{l,0}(-\dot{m}_{break,0})}$	Non-dimensionalized subcooled liquid field volume flow due to mass outflow
$C_{1,l}^*$	$C_{1,l} / C_{1,l,0}$	$C_{1,l} = \frac{\partial P / \partial u_l _{v_l}}{\sum_{k=l,m} (\rho_k V_k / \partial P / \partial v_k _{u_k})}$
$C_{1,m}^*$	$C_{1,m} / C_{1,m,0}$	$C_{1,m} = \frac{\partial P / \partial u_m _{v_m}}{\sum_{k=l,m} (\rho_k V_k / \partial P / \partial v_k _{u_k})}$
$C_2^*$	$C_2 / C_{2,0}$	$C_2 = \frac{1}{\sum_{k=l,m} (\rho_k V_k / \partial P / \partial v_k _{u_k})}$

The result of scaling analysis for the blowdown phase is summarized in Table II, which compares the non-dimensional coefficients in the mass and energy equations for the three-loop Westinghouse PWR and ROSA/LSTF SB-CL-02. The scaling factor, which is the ratio of non-dimensional parameters between the PWR and the experiment, is shown in the last column of Table 2. As seen in the table, scaling factor for  $\Psi_2$ , the ratio of pressure change due to change in specific energy of the subcooled liquid mass outflow to the reference pressure, is 0.98. The value of near 1.0 indicates the phenomenon is scaled excellently. In the same token, ratio of pressure change, due to change in specific volume of the subcooled liquid from mass outflow, to the reference pressure,  $\Psi_{10}$ , is also scaled excellently. The dimensionless group,  $\Psi_{13}$ , ratio of integrated mass flow to reference mass, shows a scaling factor of 1.47, which is in the range of 1/2 to 2. The phenomenon is still well scaled. A scale distortion is seen in the ratio of pressure change due to change in specific energy of the saturated field from heat transfer, to the reference pressure ( $\Psi_6$ ) as the scaling factor reaches 3.6. This distortion is due to the difference in the steady state operation between the PWR and ROSA. In ROSA, the steady state power is 14% of the scales power due to the power limitation for the facility (=10 MW). In order to achieve the same loop temperatures, the loop flow was also set at 14% of the scaled PWR value. The transient was initiated by a break opening followed by power transition to decay heat curve and the acceleration of pump speed until it reaches the expected coast down speed. After that, the pump follows the coast down curve. The scale distortion from this difference appears to impact marginally as the magnitude of  $\Psi_6$  is smaller than  $\Psi_{13}$  in the analysis. The mass depletion during the blowdown phase is slower in PWR than in ROSA but is comparable.

**Table II: Summary of Dimensionless Parameters during Blowdown**

Dimensionless Group	Algebraic form	Physical Meaning	PWR	ROSA	PWR/ROSA
$\Psi_2$	$\frac{C_{1,l,0}(h_{break} - u_l)\dot{m}_{break,0}t_0}{P_0}$	Ratio of pressure change, due to change in specific energy of the subcooled liquid mass outflow, to the reference pressure	4.52E-03	4.62E-03	0.98
$\Psi_6$	$\frac{C_{1,m,0}\dot{q}_{net,0}t_0}{P_0}$	Ratio of pressure change, due to change in specific energy of the saturated field from heat transfer, to the reference pressure	-9.73E-02	-2.71E-02	3.60
$\Psi_{10}$	$\frac{C_{2,0}v_{l,0}\dot{m}_{break,0}t_0}{P_0}$	Ratio of pressure change, due to change in specific volume of the subcooled liquid from mass outflow, to reference pressure	-3.08E-02	-2.97E-02	1.04
$\Psi_{13}$	$\frac{\dot{m}_{break,0}t_0}{M_0}$	Ratio of integrated mass flow to reference mass	2.11E-01	1.43E-01	1.47

### 3.2. Natural circulation phase

After the blowdown phase is natural circulation phase, where the RCS pressure is stable and controlled by the heat transfer to the steam generator secondary side. In this phase, the primary RCS system is saturated and could be modeled with one field of two-phase mixture as shown in Figure 5. The transient behaviors of interest for the natural circulation phase are the depressurization rate and the mass inventory of the RCS. Another phenomenon of interest is the system momentum balance that controls the flow rate in the natural circulation.



Figure 5. Schematic of control volume in the natural circulation phase.

The mass and energy governing equations are the same as those used for the blowdown phase, but they are further simplified to one field. The details of derivation are skipped. The final non-dimensionalized equations governing the mass and the pressure are presented.

Mass equation:

$$\frac{dM^*}{dt^*} = \Psi_{13}(-\dot{m}_{break}^*) \quad (19)$$

Pressure equation:

$$\frac{dP^*}{dt^*} = \Psi_5 C_{1,m}^* I_{b,m}^* + \Psi_6 C_{1,m}^* I_{c,m}^* + \Psi_{11} C_2^* I_m^* \quad (20)$$

Definition of non-dimensional coefficients in Eq. (19) and Eq. (20) is given in Table III. The result of scaling analysis is summarized in Table IV. As seen in the summary table, dimensionless parameters,  $\Psi_5$ ,  $\Psi_{11}$ , and  $\Psi_{13}$  are well scaled. The dimensionless parameter,  $\Psi_6$ , the ratio of pressure change due to change in specific energy of the saturated field from heat transfer to the reference pressure, shows strong distortion. This distortion is due to the difference in the heat transfer rate from the primary to the secondary side of steam generators. It is believed that two factors contributed to this distortion. One factor is the hot leg enthalpy at the beginning of natural circulation phase. Because the reactor coolant pump flow in ROSA operated at the 14% of the scaled rate during the steady state, while accelerated to the coast down curve following the initiation of the transient, combined with the delayed reactor trip, the upper plenum and hot leg stays hot for ROSA and the higher pressure in ROSA at the beginning of natural circulation phase. Second factor is the main steamline safety valve operation in ROSA. When the valve opens, the release rate is high enough to drop the secondary side so that the valve closes. The valve repeated this cycle which is in contrast to how Westinghouse three-loop PWR secondary side behaves. The difference then is the heat transfer rate from the primary to the secondary side. This difference, though notable, ends with the equilibration of the primary and the secondary pressures. At this point the heat transfer direction reverses as the primary pressure becomes lower than the secondary pressure. To address the concern of the steam generator heat transfer performance in ROSA-IV validation, additional validation against integral effects test dedicated to the natural circulation phase, ROSA ST-NC-02, was performed [24], and satisfactory validation results support the capability of the WCOBRA/TRAC-TF2 code to simulate the natural circulation phase of SBLOCA in a PWR.

**Table III: Definition of Non-dimensional Parameters in the Natural Circulation Phase**

Non-dimensionalized Parameters	Algebraic form	Note
$I_{b,m}^*$	$\frac{I_{b,m}}{I_{b,m,0}} = \frac{\dot{m}_{break}(h_{out} - u_m)}{\dot{m}_{break,0}(h_{out} - u_m)_0}$	Non-dimensionalized saturated liquid energy change due to mass outflow
$I_{c,m}^*$	$\frac{I_{c,m}}{I_{c,m,0}} = \frac{\dot{q}_{net,m}}{\dot{q}_{net,m,0}}$	Non-dimensionalized heat transfer
$\Pi_m^*$	$\frac{\Pi_m}{\Pi_{m,0}} = \frac{v_m(-\dot{m}_{break})}{v_{m,0}(-\dot{m}_{break,0})}$	Non-dimensionalized saturated field volume flow due to mass outflow
$C_{1,m}^*$	$C_{1,m} / C_{1,m,0}$	$C_{1,m} = \frac{\partial P / \partial u_m _{v_m}}{\rho_m V_m}$
$C_{2,m}^*$	$C_{2,m} / C_{2,m,0}$	$C_{2,m} = \frac{1}{\rho_m V_m / \partial P / \partial v_m _{u_m}}$

**Table IV: Summary of Dimensionless Parameters during Natural Circulation**

Dimensionless Group	Algebraic form	Physical Meaning	PWR	ROSA	PWR/ROSA
$\Psi_5$	$\frac{C_{1,m,0}(h_{break} - u_m)\dot{m}_{break,0}t_0}{P_0}$	Ratio of pressure change, due to change in specific energy of the saturated field from mass outflow, to the reference pressure	7.96E-03	6.78E-03	1.17
$\Psi_6$	$\frac{C_{1,m,0}\dot{q}_{net,0}t_0}{P_0}$	Ratio of pressure change, due to change in specific energy of the saturated field from heat transfer, to the reference	4.32E-02	-1.24E-03	-34.80
$\Psi_{11}$	$\frac{C_{2,m,0}v_{m,0}\dot{m}_{break,0}t_0}{P_0}$	Ratio of pressure change, due to change in specific volume of the saturated field from break outflow, to reference pressure	-5.68E-02	-4.85E-02	1.17
$\Psi_{13}$	$\frac{\dot{m}_{break,0}t_0}{M_0}$	Ratio of integrated mass flow to reference mass	2.92E-01	2.56E-01	1.14

The top-down scaling of the system momentum balance is based on the methodology developed by Ishii and Kataoka [12] for the two-phase natural circulation system and the momentum balance analysis for APWR. The details of the analysis are not provided here. However the results of top-down scaling analysis of system momentum balance indicate that all dimensionless groups show the scaling factors in between 0.5 and 2.0. Thus, the ROSA/LSTF is scaled well to the Westinghouse three-loop PWR in term of the momentum balance through the closed system as well as from the mass and energy balances in the natural circulation phase.

### 3.3. Loop seal clearance phase

The governing equations for the mass and the pressure in loop seal clearance phase are the same as those of the natural circulation phase. The final non-dimensionalized equations governing the mass and the pressure are Eq. (19) and Eq. (20) and the definition of non-dimensional coefficients is given in Table III.

The non-dimensional coefficients in the mass and energy equations for the PWR and ROSA SB-CL-02 are compared similarly as Table IV. The ratio of non-dimensional parameters,  $\Psi_5$ ,  $\Psi_6$ ,  $\Psi_{11}$ ,  $\Psi_{13}$ , as PWR/ROSA, is found to be 0.74, 0.51, 0.63, and 0.65, respectively. Thus, no scale distortion of mass and depressurization in the loop seal clearance phase is found.

The hydrostatic head in the RCS system in the loop seal clearance phase determines the mixture level in the core and thus the rod cladding temperature. A top-down scaling analysis with the hydrostatic head in the RCS system as the driving force in loop seal clearance phase has been performed. The details of the analysis are not provided here. The analysis results show that the parameters regarding hydrostatic head in the RCS system are well scaled.

### 3.4. Boil-off phase

The boil-off phase is the phase the vessel mixture level continues to decrease due to the boil off the remaining liquid inventory until the sufficient ECCS injection. The governing equations for the mass the pressure in boil-off phase are the same as those of the natural circulation and loop seal clearance phases.

The non-dimensional coefficients in the mass and energy equations for the PWR and ROSA SB-CL-02 are compared similarly as Table IV. The ratio of non-dimensional parameters,  $\Psi_5$ ,  $\Psi_6$ ,  $\Psi_{11}$ ,  $\Psi_{13}$ , as PWR/ROSA, are 0.78, 1.25, 0.85, and 0.96, respectively. No significant scale distortion is found. The scale distortion of the values of  $\Psi_6$  in the blowdown and natural circulation phases disappeared in this phase, which further indicates that the distortion is caused by the special pump and steam generator operation in the ROSA test.

### 3.5. Core recovery phase

The core recovery stage starts when the RCS pressure drops below the accumulator pressure and thus the accumulator injects the cold water into the RCS. The injection further reduces the RCS pressure and provides sufficient water to cool the reactor core. The peak cladding temperature has occurred at the end of boil-off phase. Thus, the core recovery phase is of less interest for the LOCA evaluation model focusing on assessing peak cladding temperature. No top-down scaling analysis is provided for the core recovery phase.

## 4. CONCLUSIONS

The top-down scaling in blowdown, natural-circulation, loop seal clearance, and boil-off phases in a ROSA-IV/LSTF SBLOCA test, SB-CL-02, was investigated relative to an equivalent three-loop Westinghouse PWR SBLOCA transient. SB-CL-02 has a 2.5% break at the bottom of the cold leg. This test was selected since this break size is the closest among the available tests to the limiting break size for the three-loop Westinghouse PWR. The scale distortion was investigated using the top-down scaling method used for AP600 and for US-APWR.

The quantitative top-down scaling analysis result indicated that most of the dimensionless parameters in the governing equations for the system mass and the pressure are well scaled in the blowdown, natural circulation, loop seal clearance, and the boil-off stages. There are small scale distortions in the natural circulation originating from the atypical steady state and transient initiation of ROSA-IV test SB-CL-02 due to the power limitation for the ROSA/LSTF facility, and the distortion disappears in the later phases of the transient. Additional validation against ROSA ST-NC-02 test was provided in the FSLOCA topical report to address the natural circulation phase. Further top-down scaling analysis on the system momentum balance in the natural circulation phase and the hydrostatic head in the loop seal clearance phase shows the parameter in the governing equations all are well scaled.

The bottom-up scaling analysis examined the pertinent loop geometry and expected flow conditions for the break flow during the blowdown phase, the counter-current flow limit (CCFL) in the steam generator (SG) U-tube, CCFL in the SG/hot leg, and the residual liquid in cross-over leg in the loop seal clearance phase were shown in Full Spectrum LOCA EM topical report. The bottom-up result indicated that there is no significant scale distortion in ROSA-IV SB-CL-02 test.

Both the top-down and bottom-up scaling analyses demonstrated that the ROSA-IV tests are well scaled IETs for examining the behavior of Westinghouse three-loop PWRs under the SBLOCA transient conditions, and are uniquely suited for the validation of WCOBRA/TRAC-TF2 for the application to SBLOCA analysis.

## REFERENCES

1. C. Frepoli, et al., "Realistic LOCA Evaluation Methodology Applied to the Full Spectrum of Break Sizes (FULL SPECTRUM LOCA Methodology)" WCAP-16996-NP, Westinghouse Electric Company (2010).
2. J. W. Spore, J. S. Elson, S. J. Jolly Woodruff, T. D. Knight, J. C. Lin, R. A. Nelson, K. O. Pasamehmetoglu, R. G. Steinke, C. Unal, J. H. Mahaffy and C. Murray, "TRAC M/FORTRAN 90 (VERSION 3.0) Theory Manual," LA UR 00 910 (2000).
3. Regulatory Guide 1.203, "Transient and Accident Analysis Methods," USNRC (2005).
4. NUREG-0800, "Standard Review Plan - 15.0.2 Review of Transient and Accident Analysis Methods", USNRC (2005).
5. Regulatory Guide 1.157, "Best-Estimate Calculations of Emergency Core Cooling System Performance," USNRC (1989).
6. Bajorek, S. M., et al., "Code Qualification Document for Best Estimate LOCA Analysis," WCAP-12945-NP-A, Westinghouse Electric Company (1998).
7. The ROSA-IV group, ROSA-IV Large Scale Test Facility (LSFT) System Description. JAERI-M 84-237, JAERI (1985).
8. "Scaling Analysis for US-APWR Small Break LOCAs," UAP-HF-10289-NP (R0), Mitsubishi Heavy Industries, Ltd. (2010).
9. E. Buckingham, "On physically similar systems; illustrations of the use of dimensional equations." *Phys. Rev.*, **4**, pp.345-376 (1914).
10. R. P. Rose, "Heat Transfer Problem Associated with the LOFT (Loss of Fluid Test) Program", *Proc. ASME-AIChE Heat Transfer Conf.*, Los Angeles, California, August 8-11 (1965).
11. W.A. Carbiener, R.A. Chudnik, "Similitude Considerations for Modeling Nuclear Reactor Blowdowns," *Transactions of American Nuclear Society*, **12**, p.361 (1969).
12. M. Ishii, I. Kataoka, "Scaling Criteria for LWR's Under Single-Phase and Two-Phase Natural Circulation", ANL-83-32, NUREG/CR-3267, Argonne National Laboratory (1983).
13. A.N. Nahavandi, F.S. Castellana, E.A. Moradkhanian, "Scaling Laws for Modeling Nuclear Reactor Systems," *Nuclear Science and Engineering*, **72**, pp.75-83 (1979).
14. N. Zuber, Problems in Modeling of Small Break LOCA, NUREG-0724 (1980).
15. N. Zuber, et al., "An Integrated Structure and Scaling Methodology for Severe Accident Technical Issue Resolution: Development of Methodology," *Nuclear Engineering and Design*, **186**, pp. 1-21 (1998).
16. S. Banerjee, M. G. Ortiz, T. K. Larson, D. L. Reeder, "Scaling in The Safety of Next Generation Reactors," *Nuclear Engineering and Design*, **186**, pp. 111-133 (1998).
17. J.N. Reyes, L. Hochreiter, Scaling Analysis for the OSU AP600 Test Facility (APEX), *Nuclear Engineering and Design*, **186** pp. 53-109 (1998).
18. N. Zuber, W. Wulff, U.S. Rohatgi, I. Catton, "Application of Fractional Scaling Analysis (FSA) to Loss of Coolant Accidents (LOCA), Part 1: Methodology Development," *Proceedings of The 11<sup>th</sup> International Topical Meeting on Nuclear Reactor Thermal- Hydraulics (NURETH-11)*, Paper 153, Popes' Palace Conference Center Avignon, France, (2005).
19. Y. Kukita, Y. Anoda, and K. Tasaka, "Summary of ROSA-IV LSTF First-Phase Test Program – Integral Simulation of PWR Small-Break LOCAs and Transients," *Nuclear Engineering and Design*, **131**, pp. 101-111 (1991).
20. S. Banerjee, M. G. Ortiz, T. K. Larson, D. L. Reeder, "Top-Down Scaling Analyses Methodology for AP600 Integral Tests," INEL-96/0040 (1997).
21. W. Wulff, U.S. Rohatgi, System Scaling for the Westinghouse AP600 PWR and Related Facilities, NUREG/CR-5541 (1998).
22. Y. Koizumi, et al., ROSA-IV/LSTF 2.5% Cold Leg Break LOCA Experiment Data Report For Runs SB-CL-01, 02, and 03, JAERI-memo 62-399, JAERI (1987).
23. R.T. Lahey, F.J., Moody, The Thermal-Hydraulics of a Boiling Water Nuclear Reactor, 2<sup>nd</sup> edition, American Nuclear Society (1993).
24. N. Petkov, K. Ohkawa, and C. Frepoli, "WCobra/TRAC-TF2 Simulation of ROSA-IV/LSTF Natural Circulation Test ST-NC-02," *Proceedings of The 14<sup>th</sup> International Topical Meeting on Nuclear Reactor Thermal- Hydraulics (NURETH-14)*, Paper 592, Toronto, Canada (2011).